Electronic Supplementary Material (ESI) for Physical Chemistry Chemical Physics.


# Lead-free $CsSnCl_3$ perovskite nanocrystals: Rapid synthesis, experimental characterization and DFT simulations

Md. Shahjahan Ali, Subrata Das, Yasir Fatha Abed, and M. A. Basith*

*Department of Physics, Bangladesh University of Engineering and Technology, Dhaka-1000, Bangladesh.*

## S1 Photocatalytic dye degradation experiment

The photocatalytic efficiency of the as-prepared $CsSnCl_3$ perovskite was evaluated by the photodegradation of a well-known organic pollutant, rhodamine-B (RhB) dye in aqueous solution [1,2]. Initially, 1.2 mg of RhB was dissolved in 100 mL distilled water. Then, 4 mL of this solution was extracted and its absorbance spectrum was determined using a UV–vis spectrophotometer (UV- 2600, Shimadzu) to estimate the amount of RhB present in the solution since the intensity of the absorbance peak at 553 nm is proportional to the concentration of RhB. Thereafter, 40 mg $CsSnCl_3$ photocatalyst was added into 50 mL of this solution followed by magnetic stirring of the suspension in dark for 1 h to achieve an adsorption-desorption equilibrium between the photocatalyst nanocrystals and RhB in the solution. After that, the photocatalytic process was initiated by irradiating the solution using a solar simulator i.e. 500 W mercury-xenon lamp (Hamamatsu L8288) with an irradiance value of 100 $mWcm^{-2}$ in the visible spectrum. After 30 minutes of illumination, 4 mL of suspension was extracted and centrifuged at 5500 rpm for 10 minutes. Then, the concentration of the remaining RhB was evaluated by obtaining the absorbance spectrum of the mixture using UV-vis spectrophotometer. This same process was carried out for 4 hours at 30 minutes interval.

Corresponding author: mabasith@phy.buet.ac.bd

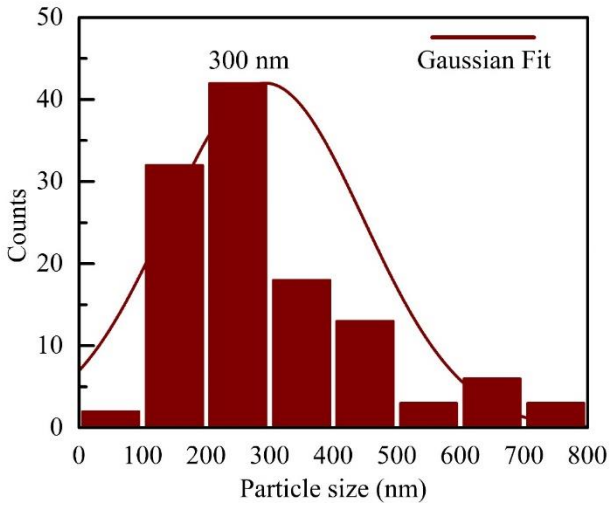


Figure S1: Histogram shows the distribution of the crystal size of $CsSnCl_3$ nanocrystals with an average of 300 nm.

Table S1: Mass and atomic percentages of $CsSnCl_3$ nanocrystals as obtained by EDX analysis.

| Element | Mass (%) (Theoretical) | Mass (%) (Experimental) | Atom (%) (Theoretical) | Atom (%) (Experimental) |
|---|---|---|---|---|
| Cs | 37.13 | 45.91 | 20 | 23.43 |
| Sn | 33.16 | 29.48 | 20 | 18.59 |
| Cl | 29.71 | 24.61 | 60 | 57.98 |
| Total | 100 | 100 | 100 | 100 |

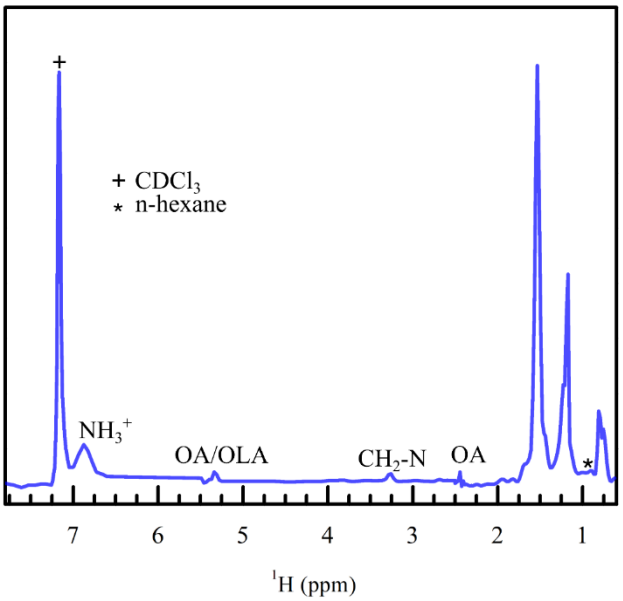


Figure S2: 1D $^{1}$H NMR spectrum of $CsSnCl_3$ perovskite nanocrystals. The resonance peaks of $CDCl_3$ solvent (marked by + sign) and n-hexane, used for washing nanocrystals (denoted by * sign), along with the characteristic resonant peaks of oleic acid (OA), oleylamine (OLA) are shown in the spectrum.

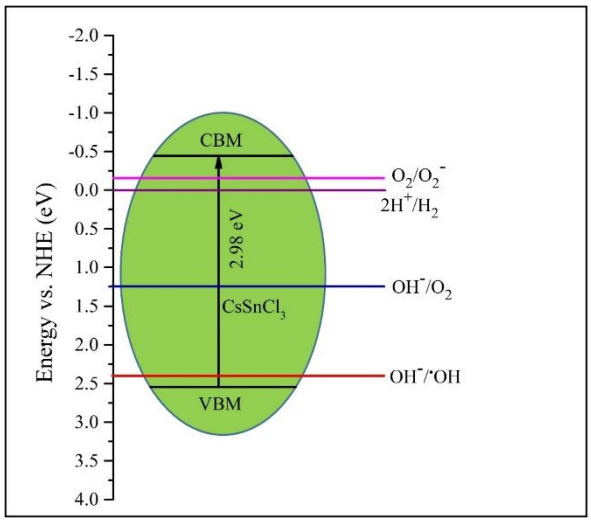


Figure S3: Band edge positions adopted from Mulliken electronegativity approach conveying the potential use of fabricated $CsSnCl_3$ as an efficient photocatalyst.

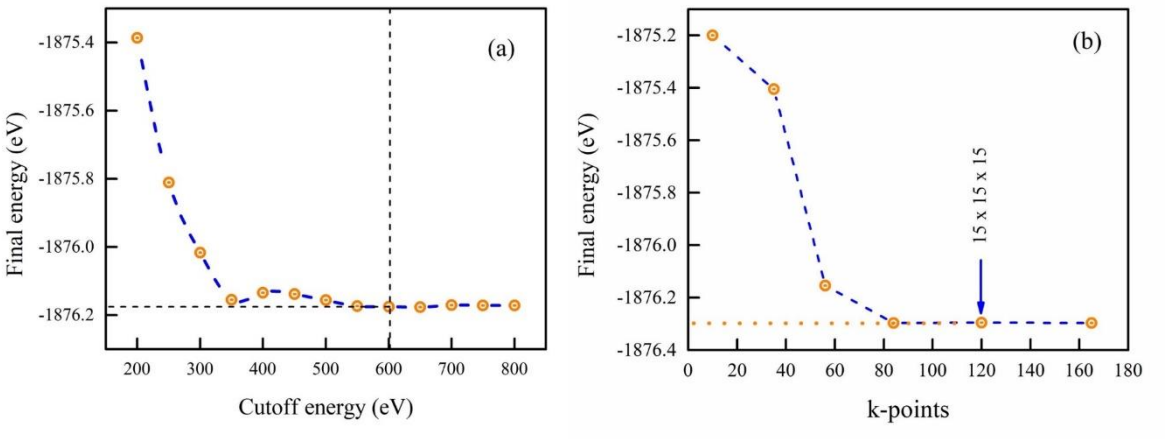


Figure S4: (a) Plane-wave cutoff energy convergence for structural optimization, shows 600 eV is sufficient to converge the ground state energy, (b) k-point point grid variation for structure optimization of $CsSnCl_3$ demonstrate that 15 x 15 x 15 k-point grid is sufficient to obtain the ground state energy.

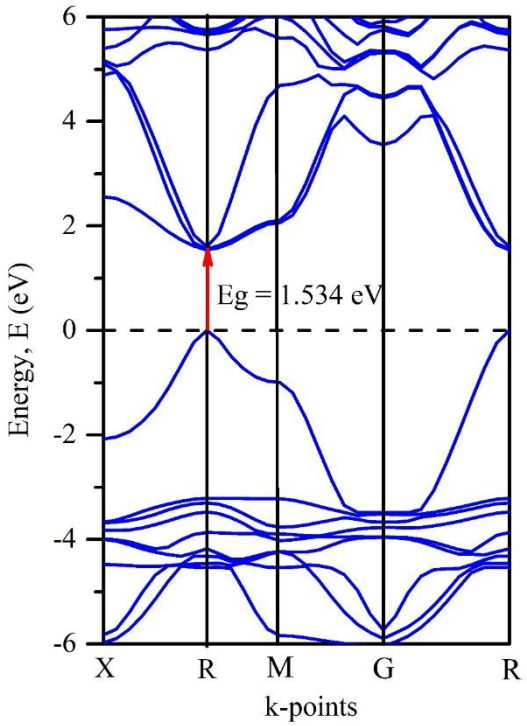


Figure S5: Electronic band structure calculation of $CsSnCl_3$ nanocrystals obtained by using HSE06 functional.

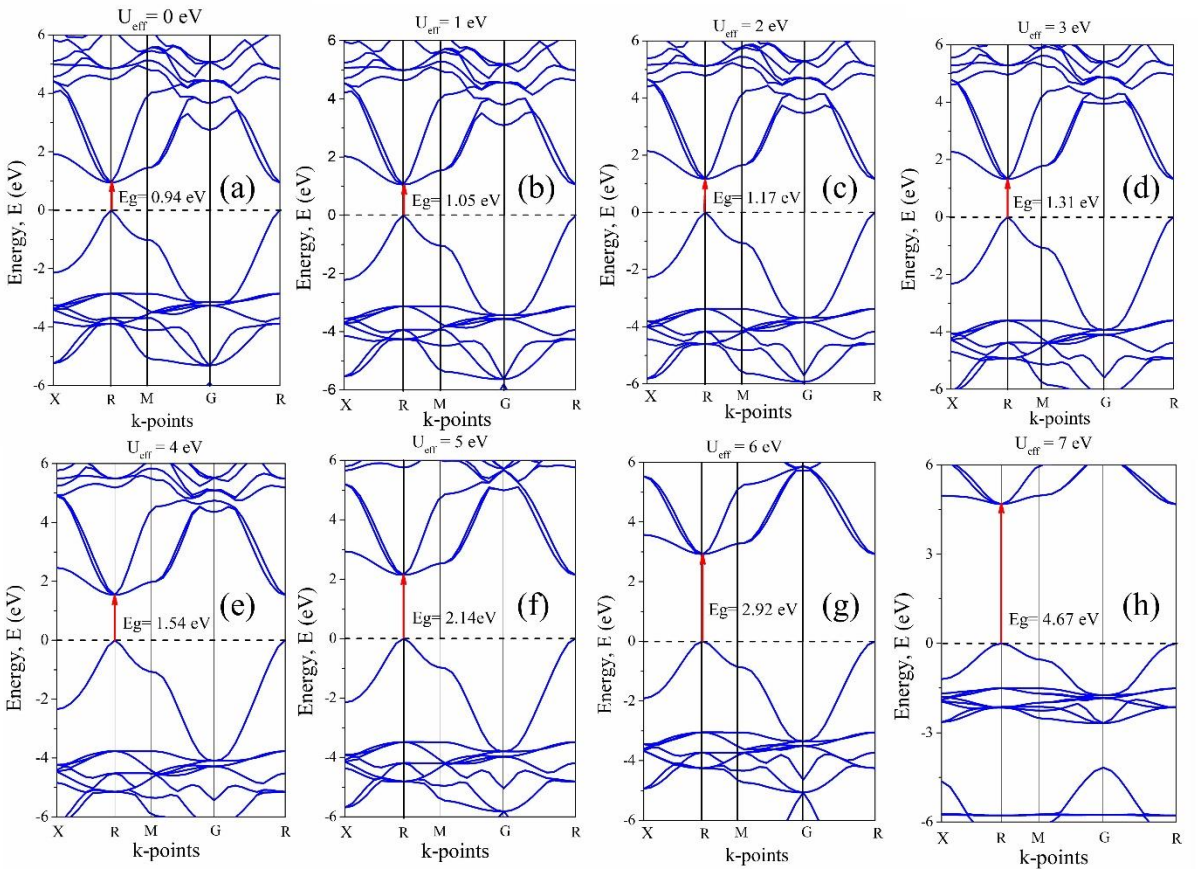


Figure S6: Electronic band structure of metal halide perovskites $CsSnCl_3$ for (a) $U_{eff}$ = 0 eV, (b) $U_{eff}$ = 1 eV, (c) $U_{eff}$ = 2 eV, (d) $U_{eff}$ = 3 eV, (e) $U_{eff}$ = 4 eV, (f) $U_{eff}$ = 5 eV, (g) $U_{eff}$ = 6 eV, (h) $U_{eff}$ = 7 eV. Here the bandgap widens with the increase of $U_{eff}$ due to the localization improvement in the Cl 3p and Sn 5p orbitals.

**Mulliken population analysis**

We have calculated the effective atomic charge, bond population and bond length in as-synthesized $CsSnCl_3$ crystal structure via Mulliken population analysis in order to gain insight into the distribution of electrons among different parts of its atomic bonds, bond covalency and bond strength. Notably, the Mulliken effective charge, Q(α) of an atom α can be calculated by the following equation [3]

$$Q(\alpha) = \sum_{k} \omega_k \sum \sum_{\mu}^{\text{on } \alpha} \sum_{v} P_{\mu v}(k) S_{\mu v}(k) \qquad (1)$$

where $P_{\mu v}$ is an element of the density matrix and $S_{\mu v}$ denotes the overlap matrix. The bond population, P(αβ) between two atoms α and β can be obtained by the following expression [1]

$$P(\alpha\beta) = \sum_{k} \omega_k \sum_{\mu}^{\text{on } \alpha} \sum_{v}^{\text{on } \beta} 2P_{\mu v}(k) S_{\mu v}(k) \quad (2)$$

The Mulliken effective charges of individual atoms of $CsSnCl_3$ calculated for different values of $U_{eff}$ have been provided in ESI Table S2. It can be observed that for all values of $U_{eff}$, the calculated Mulliken effective charges of the individual Cs, Sn, and Cl atoms are reasonably smaller than their formal ionic charges i.e. +1, +2, and -1, respectively which indicates the presence of covalent bonding in $CsSnCl_3$. Moreover, Table S2 in ESI demonstrates that the absolute value of Cs, Sn and Cl atoms' effective charges increased with the enhancement of $U_{eff}$. It is well-known that large Mulliken effective charge of an atom is associated with its low level of covalency and vice versa. Hence, we may infer that the degree of bond covalency in $CsSnCl_3$ perovskite gradually decreased because of the enhanced effect of on-site Coulomb interaction.

ESI Table S2 also presents the bond populations and bond lengths of Sn-Cl bond in $CsSnCl_3$ as determined for $U_{eff}$ = 0 to 7 eV. The positive and reasonably high value of bond population suggests that the Sn-Cl bond is prominently covalent. However, the bond population decreased with increasing $U_{eff}$ which is another indication for the influence of Coulomb repulsion to reduce the bond covalency. Interestingly, this conjecture has been further justified by the calculated Sn-Cl bond lengths for different values of $U_{eff}$ as tabulated in ESI Table S2. The increment of Sn-Cl bond length with increasing $U_{eff}$ can be attributed to the decreased bond population and consequently, the reduction in bond covalency.

Table S2: Mulliken effective charges of individual atoms, bond populations and bond lengths of $CsSnCl_3$ for different values of $U_{eff}$ obtained via Mulliken population analysis.

| Atom | $U_{eff}$ = 0 eV | $U_{eff}$ = 1 eV | $U_{eff}$ = 2 eV | $U_{eff}$ = 3 eV | $U_{eff}$ = 4 eV | $U_{eff}$ = 5 eV | $U_{eff}$ = 6 eV | $U_{eff}$ = 7 eV |
|---|---|---|---|---|---|---|---|---|
| Mulliken effective charge | | | | | | | | |
| Cs | 0.90 | 0.90 | 0.89 | 0.89 | 0.89 | 0.92 | 0.96 | 0.97 |
| Sn | 0.76 | 0.81 | 0.91 | 0.91 | 0.97 | 1.08 | 1.23 | 1.58 |
| Cl | -0.55 | -0.57 | -0.60 | -0.60 | -0.62 | -0.67 | -0.73 | -0.85 |
| Bond | Bond population | | | | | | | |
| Sn-Cl | 0.35 | 0.34 | 0.33 | 0.33 | 0.32 | 0.32 | 0.31 | 0.22 |
| Bond | Bond length (Å) | | | | | | | |
| Sn-Cl | 2.806 | 2.802 | 2.802 | 2.802 | 2.812 | 2.869 | 2.945 | 3.173 |

**Reference**


**[1]** M. A. Basith, N. Yesmin and R. Hossain, *RSC Adv.*, 2018, **8**, 29613–29627.

**[2]** S. Das, S. Dutta, A. M. Tama and M. A. Basith, *Mater. Sci. Eng. B*, 2021, **271**, 115295.

**[3]** R. S. Mulliken, *J. Chem. Phys.*, 1955, **23**, 10-1063.